THE EFFECT OF SATURN'S RINGS ON THE UPPER-BOUNDARY INSOLATION OF ITS ATMOSPHERE

E. VAN HEMELRIJCK
Belgian Institute for Space Aeronomy, Brussels, Belgium

(Received 25 August, 1986)

Abstract. In this paper, the daily solar radiation incident at the top of Saturn's atmosphere and taking into account both the oblateness of the planet and the shadow of the ring system is calculated. It is found that the decrease of the daily insolation in winter is important near the solstices up to mid-latitudes and in the neighborhood of the equinoxes for equatorial and low latitudes. The combined effect of Saturn's rings and its flattening on the mean winter and annual daily insolations is also studied. The numerical results show that the mean wintertime insolation falls gradually in the (0–20°) latitude region to a peak value of about 50%. Beyond 20° the loss of insolation decreases and from approximately 45° up to polar region latitudes the decrease reaches a practically constant level of 35%. The mean annual daily insolation is maximally reduced by about 20% at localities of 20°.

1. Introduction

The effect of the major rings (A, B, and C) on the direct solar radiation at the top of Saturn's atmosphere has been calculated and briefly discussed by Brinkman and McGregor (1979). The oblateness of the planet was also taken into account.

In their paper, the data for the Saturnian ring system (inner radius, outer radius and optical depth) were taken from Allen (1963) and Cook and Franklin (1973). Since the encounter of the Voyager spacecrafts with the planet, new and more accurate data for the distances from Saturn and the optical thickness are available. Although most of the values used by Brinkman and McGregor (1979) are close to the more recent ones, it is to be emphasized that the B-ring optical depth is found to be higher than previously published values, the difference being of the order of 20 (inner B-ring) to approximately 80% (outer B-ring) (Esposito *et al.*, 1983). The exact value of the effective B-ring optical thickness is, however, poorly determined due to the presence of relatively small regions of extremely low optical depths within an overall highly opaque layer (Smith *et al.*, 1981).

The present work differs from that of Brinkman and McGregor (1979) in that the rings are divided into two (A and C) or three (B) regions of different optical thicknesses and that we also took into consideration the Cassini division which has been ignored by the above mentioned authors. (The other rings are neglected because they are assumed to be transparent). Moreover, our calculations are based on the data recently published by Esposito *et al.* (1983). It has also to be noticed that in the paper of Brinkman and McGregor (1979) some expressions were slightly in error.

In a first section we briefly present the calculation scheme for the upper-boundary insolation including the flattening effect and the shadow effect of the ring system.

Earth, Moon, and Planets **38** (1987) 217–235.

Then, taking into account the planetary and orbital data of Saturn, we determine the daily insolation and the mean (summer, winter or annual) daily insolations. In the Figures, the incident solar radiations are given in calories per square centimeter per Saturnian day; insolation values expressed in Watt per square meter may be obtained by multiplying the unit used by a factor of about 0.484.

2. Calculation Scheme for the Daily Insolation

In calculating the ring contribution, the rings are treated as infinitely thin, homogeneous annuli and are assumed to be in the equatorial plane.

We have followed the method of Brinkman and McGregor (1979) in adopting a rectangular coordinate system: the z-axis coincide with the spin axis of the planet, the y-axis is perpendicular to the Sun's rays and the x-axis is defined so as to form a right handed coordinate system. The origin O is located in the center of the planet and $z = 0$ represents the expression of the equator.

The coordinates of a point P on the rings may now be written under the following forms:

$$x = R \cos \alpha, \tag{1}$$

$$y = R \sin \alpha, \tag{2}$$

$$z = 0; \tag{3}$$

where R is the radial distance (in units of Saturn radii $R_S = 60000$ km) of P from the origin O and α is the angle between the line connecting the point to the origin and the x-axis.

For an oblate planet, characterized by a flattening f, the line throughout P and parallel to the Sun's rays intersects the planet at the point S, the coordinates of which are given by

$$x_S = z_S \cot \delta_\odot + R \cos \alpha, \tag{4}$$

$$y_S = R \sin \alpha, \tag{5}$$

$$z_S = \{ - R \cos \alpha \cot \delta_\odot \pm \{(R \cos \alpha \cot \delta_\odot)^2 - \\ - [\cot^2 \delta_\odot + (1 - f)^{-2}] (R^2 - 1)\}^{1/2}\}/[\cot^2 \delta_\odot + (1 - f)^{-2}], \tag{6}$$

where $\delta_\odot$ is the solar declination.

Expression (6) can also be written as

$$z_S = \{ - R \cos \alpha \cot \delta_\odot) \pm [(R \cos \alpha \cot \delta_\odot)^2 - \\ - (1.256 + \cot^2 \delta_\odot) (R^2 - 1)]^{1/2}\}/(1.256 + \cot^2 \delta_\odot), \tag{7}$$

where the factor 1.256 represents, in a very good approximation, the numerical value of the expression $(1 - f)^{-2}$ (see Table I).

In (6) or (7) the smallest absolute value has to be taken as z-coordinate, the largest one representing the theoretical intersection on the unilluminated side of the planet.

Furthermore, it is easy to see that the planetocentric latitude φ' and the longitude λ (with respect to the rotating x-axis) of the intersection point can be calculated using the relations

$$\varphi' = \tan^{-1} [z_S/(x_S^2 + y_S^2)^{1/2}], \tag{8}$$

$$\lambda = \tan^{-1} (y_S/x_S). \tag{9}$$

The shadow profiles, for a solar declination $\delta_\odot$ (taken to be constant over a Saturnian day) and a radial distance R, can be determined by combining (4), (5), (7), (8), and (9). The Sun's rays throughout points on the ring system for which

$$\alpha > \cos^{-1} \{(\tan \delta_\odot/R)[(1.256 + \cot^2 \delta_\odot)\ (R^2 - 1)]^{1/2}\} \tag{10}$$

do not intersect the planet. After rearrangement, Equation (10) can also be written in a more simplified form as

$$\alpha > \cos^{-1} [(1 + 1.256 \tan^2 \delta_\odot)\ (1 - 1/R^2)]^{1/2}. \tag{11}$$

The expression of a plane parallel to the equator, in terms of the planetocentric latitude φ' can be written as

$$z = \pm (1.256 + \cot^2 \varphi')^{-1/2} \tag{12}$$

where the plus sign is used for the northern hemisphere ($\varphi' > 0$), and the minus sign is taken for the southern one ($\varphi' < 0$). The above mentioned plane intersects the shadow profiles for angles α which are given by

$$\alpha = \pm \cos^{-1} \{[(1.256 + \cot^2 \delta_\odot)\ (1.256 + \cot^2 \varphi')^{-1} + (R^2 - 1)]/2R \cot \delta_\odot\ (1.256 + \cot^2 \varphi')^{1/2}\}. \tag{13}$$

Finally, relationships (4), (5), (7), (9), and (13) allow the integration angles for the calculation of the daily insolation to be determined for any declination angle $\delta_\odot$ (or for any specific day) as a function of the planetocentric latitude φ' and the radial distance R.

The instantaneous insolation (I) of the outer planets, neglecting the oblateness effect or any other effect, may be expressed (see, e.g., Ward, 1974; Vorob'yev and Monin, 1975; Levine *et al.*, 1977; Van Hemelrijck, 1982a, b, c, 1983a) as

$$I = S \cos z', \tag{14}$$

with

$$S = S_0/r_\odot^2 \tag{15}$$

and

$$r_\odot = a_\odot(1 - e^2)/(1 + e \cos W). \tag{16}$$

In expressions (14) to (16) S, z', S_0, $a_\odot$, e, and W are, respectively, the solar flux at an heliocentric distance $r_\odot$, the zenith angle of the incident solar radiation, the solar constant at the mean Sun–Earth distance of 1 AU taken at 1.96 cal cm^{-2} $(min)^{-1}$ (Wilson, 1982), the planet's semimajor axis, the eccentricity and the true anomaly which is given by

$$W = \lambda_\odot - \lambda_P, \tag{17}$$

where $\lambda_\odot$ and λ_P are the planetocentric longitude of the Sun (called solar longitude in the figures) and the planetocentric longitude of the planet's perihelion.

For a spherical planet, the cosine of the zenith angle z' may be written as

$$\cos z' = \sin \varphi' \sin \delta_\odot + \cos \varphi' \cos \delta_\odot \cos h, \tag{18}$$

where h is the local hour angle of the Sun; $\delta_\odot$ can be computed from the relation:

$$\sin \delta_\odot = \sin \epsilon \sin \lambda_\odot. \tag{19}$$

The daily insolation I_D (see also Van Hemelrijck, 1983b, 1985b) can now be obtained by integrating relation (14) over time during the light time of the day and is given by:

$$I_D = (ST/\pi)\,(h_0 \sin \varphi' \sin \delta_\odot + \sin h_0 \cos \varphi' \cos \delta_\odot), \tag{20}$$

where T is the sidereal day and where the local hour angle at sunrise (or sunset) h_0 may be determined from:

$$h_0 = \cos^{-1}(-\tan \delta_\odot \tan \varphi') \tag{21}$$

if

$$|\varphi'| < \pi/2 - |\delta_\odot|.$$

In regions where there is no sunrise ($\varphi' < -\pi/2 + \delta_\odot$ or $\varphi' > \pi/2 + \delta_\odot$) we have $h_0 = 0$; in regions where the Sun remains above the horizon all day ($\varphi' > \pi/2 - \delta_\odot$ or $\varphi' < -\pi/2 - \delta_\odot$), we may put $h_0 = \pi$.

Finally, the mean (summer, winter or annual) daily insolations, hereafter denoted as $(\bar{I}_D)_S$, $(\bar{I}_D)_W$ and $(\bar{I}_D)_A$ respectively, may be found by integrating relation (20) within the appropriate time limits, yielding the total insolation over a season or a year, and by dividing the obtained result by the corresponding length of the summer (T_S) or winter (T_W) or tropical year ($T_)$). For the calculation of T_S or T_W we refer to e.g. Van Hemelrijck (1982c).

In this paper, and for the northern hemisphere, the summer is arbitrary defined as running from vernal equinox over summer solstice to autumnal equinox and spanning 180°; on the other hand, it is obvious that $\lambda_\odot = 180°$ and $\lambda_\odot = 360°$ mark the beginning and the end of the winter period. In the southern hemisphere, the solar longitude intervals (0–180°) and (180–360°) divide the year into astronomical winter and summer.

In the case of an oblate planet, there is an angle $v = \varphi - \varphi'$, the so-called angle of the vertical, between the planetographic latitude(φ) and the planetocentric latitude (φ'). In terms of the latter, this angle can be written as

$$v = \tan^{-1}(1.256 \tan \varphi') - \varphi'. \tag{22}$$

If we define Z as the zenith angle for an oblate planet, the following relation can be obtained by applying the formulas of spherical trigonometry (Van Hemelrijck, 1982a, b, 1983a)

$$\cos Z = \cos v \cos z' + \sin v\,(-\tan \varphi' \cos z' + \sin \delta_{\odot} \sec \varphi'). \tag{23}$$

The daily insolation of an oblate planet I_{DO} can now be obtained by integrating relation (14) within the appropriate time limits, where $\cos z'$ has to be replaced by expression (23), yielding

$$\begin{aligned} I_{DO} = (ST/\pi)\,\{&\cos v\,(h_{00} \sin \varphi' \sin \delta_{\odot} + \sin h_{00} \cos \varphi' \cos \delta_{\odot}) + \\ &+ \sin v[-\tan \varphi'\,(h_{00} \sin \varphi' \sin \delta_{\odot} + \sin h_{00} \cos \varphi' \cos \delta_{\odot}) + \\ &+ h_{00} \sin \delta_{\odot} \sec \varphi']\}, \end{aligned} \tag{24}$$

where h_{00}, the local hour angle at rising or setting of the Sun for an oblate planet, is generally slightly different from h_0. As for a spherical planet, h_{00} may be derived from Equation (23) which gives:

$$h_{00} = \cos^{-1}(-\tan \delta_{\odot} \tan \varphi), \tag{25}$$

which is similar to Equation (21).

Obviously, in areas of permanent darkness and continuous sunlight we have $h_{00} = 0$ and $h_{00} = \pi$, respectively.

The oblateness effect on the solar radiation at the top of the atmosphere of Saturn (and other planets) has been analyzed in detail by Van Hemelrijck (1982a). It has been found that the flattening causes significant variations in both the planetary-wide distribution and the intensity of the daily insolation and, of course, in the latitudinal variation of the mean daily insolations.

The shadows cast by the ring system of Saturn cause the insolation to decrease by an amount depending upon the latitude, the oblateness and the solar declination via $\cos Z$ and evidently, upon the optical depth τ of one or more than one ring (if there is no intersection or if a point on the planet is outside of any ring shadow it is clear that the optical depth equals zero).

The daily insolation $I_{DO\tau}$, taking into account both the shadow effect and the influence of the oblateness, may then be expressed (Levine *et al.*, 1977; Brinkman and McGregor, 1979; Van Hemelrijck, 1985a) as:

$$I_{DO\tau} = (ST/\pi) \int_0^{h_{00}} \cos Z \exp(-\tau \sec Z)\, \mathrm{d}h. \tag{26}$$

TABLE I

Elements of the planetary orbit of Saturn

Semimajor axis	$a_{\odot}$ (AU)	9.539
Eccentricity	e	0.05561
Longitude of perihelion	λ_P (°)	279.07
Obliquity	ϵ (°)	26.73
Oblateness	f	0.1076209
Sidereal day	T (Earth days)	0.44
Tropical year	T_0 (,,)	10759.20
Length of summer	T_S (,,)	5755.56
Length of winter	T_W (,,)	5003.64

In winter and for a given latitude it is evident that, in general, the integration interval $(0 - h_{00})$ has to be divided into two or more regions depending upon the number of rings that, during the day, casts a shadow on the latitude under consideration. Furthermore, it is also obvious that τ, figuring in expression (26), represents the optical thickness corresponding to the ring which attenuates the solar radiation.

The mean daily insolations $(\bar{I}_{DO_7})_A$, $(\bar{I}_{DO_7})_S$, and $(\bar{I}_{DO_7})_W$ may, as earlier, be found by integrating equation (26) over the appropriate time periods.

Table I represents the numerical values of the orbital and planetary data (Van Hemelrijck, 1982a; Davies *et al.*, 1983) used for the computations, whereas parameters for the ring system are given in Table II (Esposito *et al.*, 1983). It has to be pointed out that T_S and T_W, figuring in Table I, represents the lengths of the summer and winter corresponding to the northern hemisphere. For the southern one, the two values have to be interchanged.

TABLE II

Parameters of the ring system

Region	Boundaries (R_S)	Mean τ
Inner C	1.24–1.39	0.08
Outer C	1.39–1.52	0.15
Inner B	1.52–1.66	1.21
Middle B	1.66–1.72	1.76
Outer B	1.72–1.95	1.84
Cassini	1.95–2.02	0.12
Inner A	2.02–2.16	0.70
Outer A	2.16–2.27	0.57

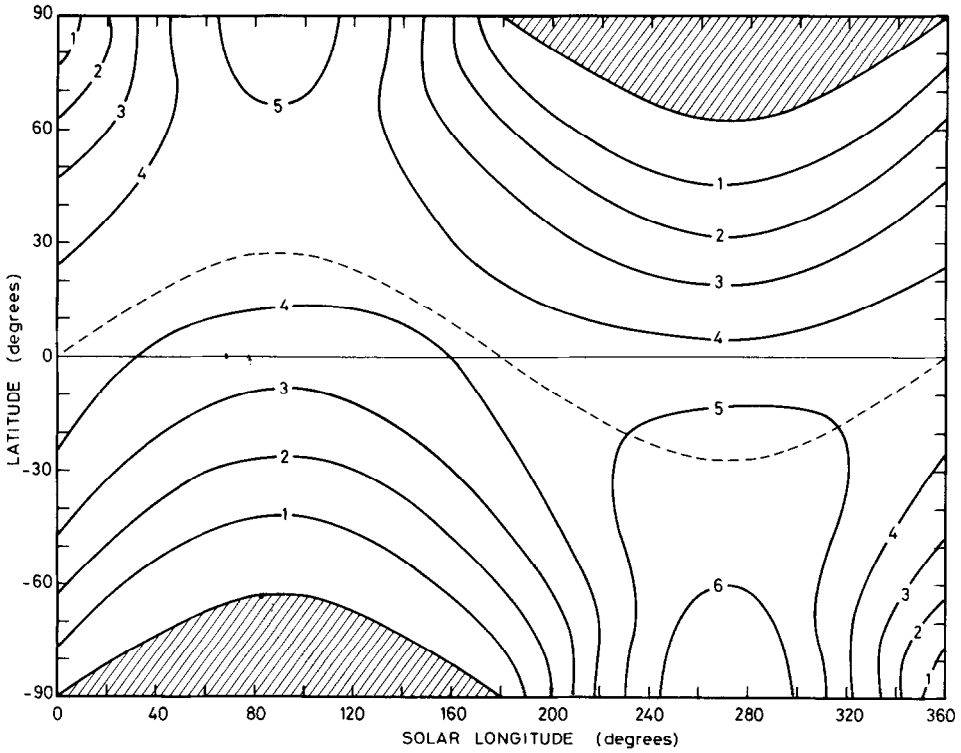

Fig. 1. Seasonal and latitudinal variation of the daily insolation at the top of the atmosphere of Saturn. The planet is assumed to be spherical and the shadow effect of the ring system is neglected. Solar declination is represented by the dashed line. The areas of permanent darkness are shaded. Values of the daily insolation in calories per square centimeter per Saturnian day are given on each curve.

3. Discussion of Calculation

3.1 Daily Insolation

For the daily insolation, as already mentioned, we have followed the method adopted by e.g. Levine *et al.* (1977) and Brinkman and McGregor (1979) in presenting our results in the form of contour maps giving the incident solar radiations in cal cm^{-2} (Saturnian day)$^{-1}$ as a function of latitude and heliocentric longitude of the Sun taken to be equal to 0° at the northern hemisphere vernal equinox.

Figure 1 illustrates the latitudinal and seasonal distribution of the daily insolation (see also Vorob'yev and Monin, 1975; Levine *et al.*, 1979). The planet is considered as a sphere and the influence of the ring system is neglected. The calculations reveal that the maximum solar radiations occur near the solstices. This is due to the fact that the perihelion position λ_p is located in the vicinity of the south summer solstice. The insolation at the solstices reaches about 5.5 (north pole) and 6.8 (south pole) cal cm^{-2} (Saturnian day)$^{-1}$. The ratio of both insolations, in terms of e and λ_p, may be

expressed (cf. Van Hemelrijck, 1982c) as

$$(I_D)_{\mathrm{NP(ss)}}/(I_D)_{\mathrm{SP(ss)}} = [(1 + e \sin \lambda_P)/(1 - e \sin \lambda_P)]^2, \tag{27}$$

where the subscripts NP, SP, and ss refer respectively to the north pole, the south pole, and the summer solstices. Expression (27) indicates that $(I_D)_{\mathrm{NP(ss)}} < (I_D)_{\mathrm{SP(ss)}}$ if $\pi < \lambda_P < 2\pi$ which is true not only for Saturn, but also for the Earth ($\lambda_P = 282°$) and Mars (248°). For the outer planets Jupiter, Uranus, and Neptune the opposite effect is found.

The ratio of the polar solar radiation at summer solstice $(I_D)_{\mathrm{P(ss)}}$ to the equatorial one $(I_D)_{\mathrm{E(ss)}}$ can be written by the well-known relationship

$$(I_D)_{\mathrm{P(ss)}}/(I_D)_{\mathrm{E(ss)}} = \pi \tan \epsilon, \tag{28}$$

stating that $(I_D)_{\mathrm{P(ss)}} > (I_D)_{\mathrm{E(ss)}}$ for $\epsilon > 17°7$. For Saturn, this ratio amounts to about 1.6. Based on the above mentioned values for the polar summer solstice insolation it follows that the corresponding equatorial insolation is approximately equal to $3.5(\lambda_\odot = 90°)$ and $4.3(\lambda_\odot = 270°)$ cal cm^{-2} (Saturnian day)$^{-1}$.

One can also determine mathematically the solar longitude intervals where $(I_D)_{\mathrm{P}} > (I_D)_{\mathrm{E}}$. Indeed, from (20) it is easy to show that

$$(I_D)_{\mathrm{P}}/(I_D)_{\mathrm{E}} = \pm \pi \tan \delta_\odot = \pm \pi \sin \epsilon \sin \lambda_\odot/(1 - \sin^2 \epsilon \sin^2 \lambda_\odot)^{1/2}; \tag{29}$$

the plus sign being used for the north pole, the minus sign for the southern one. Introducing $\epsilon = 26°73$ in Equation (29) it follows that, in the northern hemisphere, $(I_D)_{\mathrm{P}} > (I_D)_{\mathrm{E}}$ if $\lambda_\odot$ ranges from approximately 42 to 138°. In the southern hemisphere the polar daily insolation exceeds that of the equator in the approximate solar longitude interval (222–318°).

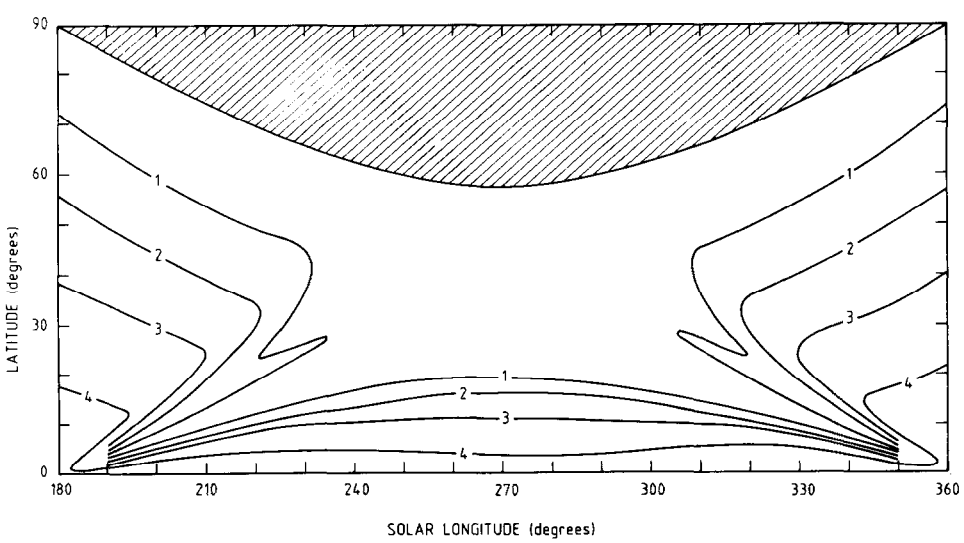

Fig. 2. Seasonal and latitudinal variation of the daily insolation (I_{DO_T}) at the top of the atmosphere of Saturn (northern winter hemisphere). Both the oblateness effect and the shadow effect of the ring system are taken into account. See Figure 1 for full explanation.

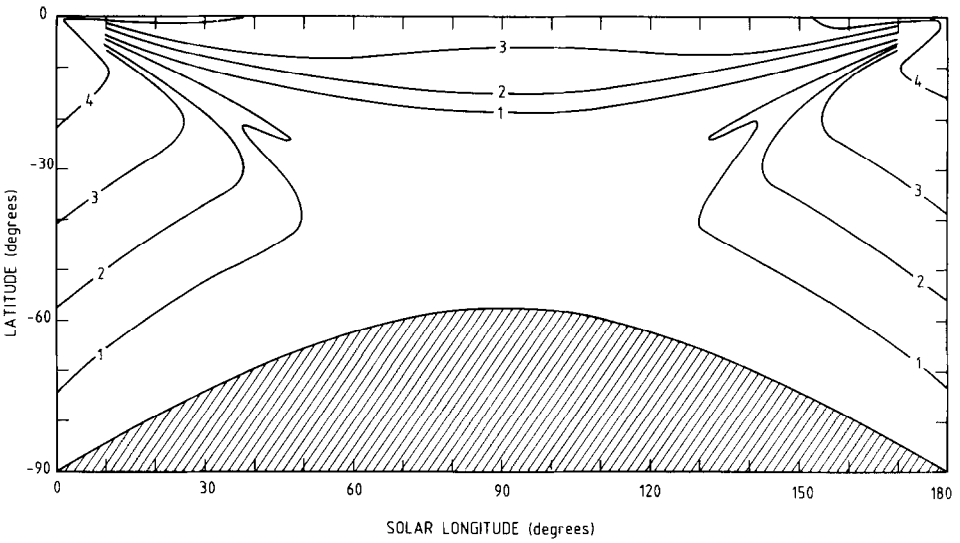

Fig. 3. Seasonal and latitudinal variation of the daily insolation (I_{DO_T}) at the top of the atmosphere of Saturn (southern winter hemisphere). Both the oblateness effect and the shadow effect of the ring system are taken into account. See Figure 1 for full explanation.

Finally in winter, as for practically all the outer planets, the iso-contours closely parallel the curve limiting the area of no sunrise. In summer, the parallelism between the insolation contours and the line bounding the zone of continuous sunlight vanishes almost completely.

The seasonal and latitudinal variation of the solar radiation at the top of the Saturnian atmosphere, taking into account both the oblateness effect and the shadow effect of the ring system, is plotted in Figures 2 (northern winter hemisphere) and 3 (southern winter hemisphere). The insolation pattern for the summer period is not plotted because it can easy be seen that the summer hemispheres are not affected by the ring system. For the influence of the oblateness on the daily solar radiation in this region we refer to Van Hemelrijck (1982a). This paper reveals that the effect of the oblateness increases the insolation over much of the summer hemisphere, especially near summer solstice, where a rise of the incident solar radiation on the order of 3% has been found. In the neighborhood of the equinoxes there is a loss of insolation which is of most importance for the mid-latitude regions.

Comparing Figure 1 with Figures 2 and 3, we find it obvious that the ring system causes the daily solar radiation to decrease over an extensive part of the winter hemisphere. This characteristic feature is studied, in more details, in Figures 4, 5, and 6 presenting the latitudinal variation (for some specific values of the solar longitude) of the ratio of the daily insolation taking into account both the shadow effect and the oblateness effect (I_{DO_T}) to the daily insolation without those effects (I_D) (full line). The ratio (I_{DO}/I_D) (dashed line) is also given.

Near the autumnal equinoxes (Figure 4), where the solar declination ($\delta_\odot$) is rather small, the shadows of the ring system are limited to equatorial latitudes and, as a

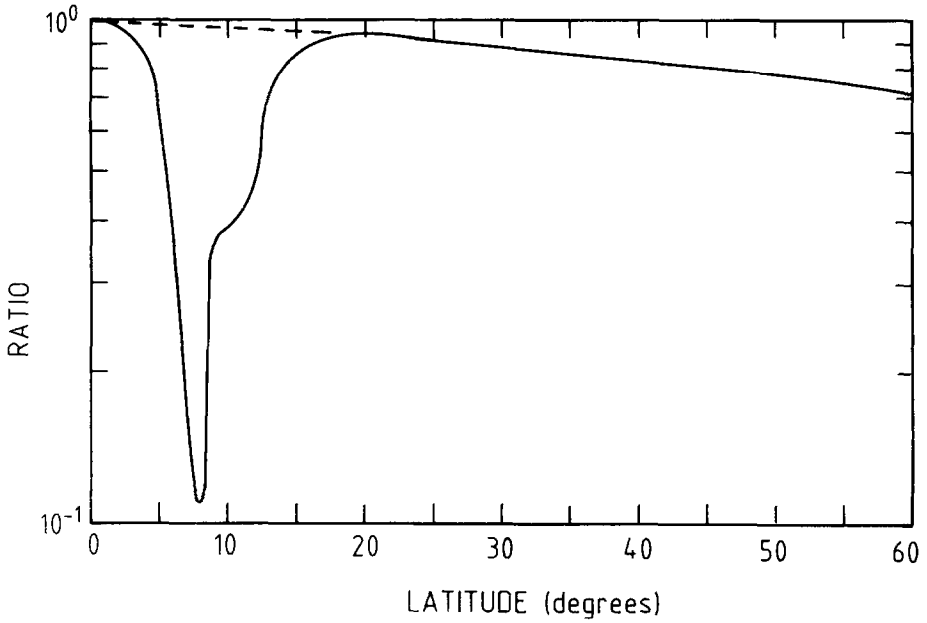

Fig. 4. Latitudinal variation in the winter hemisphere at a solar longitude of 20° (200°) of the ratio of the daily insolation with the oblateness effect and the effect of the ring system (I_{DO_T}) to the daily insolation without the above mentioned effects (I_D) (full line). The ratio (I_{DO}/I_D) is also represented (dashed curve).

consequence, the attenuation of the solar radiation is confined to this low latitudes. This phenomenon is clearly demonstrated in Figure 4 for a solar longitude of 20° (southern hemisphere) or 200° (northern hemisphere). The loss of insolation reaches a maximum at a latitude of approximately 8° and equals a factor of nearly 10. At a latitude of about 20° the curves representing the ratios (I_{DO_T}/I_D) and (I_{DO}/I_D) coincide which means that the shadow effect is no more applicable to latitudes beyond the above mentioned one and for a solar position of 20° (or 200°).

The latitudinal ratio distribution at a solar longitude between autumnal equinox and winter solstice is shown in Figure 5. The ratio of both insolations (I_D and I_{DO_T}) amounts to about 20 ($I_{DO_T}/I_D \simeq 0.05$) at localities equal to 20° latitude. Past of 40°, the influence of the ring system is either unimportant and it is exclusively the oblateness which is responsible for the reduction of the insolation (ratio $\simeq 0.76$).

The loss of the solar radiation at winter solstice in both hemispheres is even more spectacular as can be deduced from Figure 6. For example, at latitudes of 23, 29, and 38°, the corresponding ratios (I_{DO_T}/I_D) are equal to 10^{-1}, 10^{-2}, and 10^{-3}, respectively.

In winter, as for all planets, the effect of the flattening results in a more extensive polar region; the large oblateness of Saturn gives rise to a maximum difference of the two Arctic Circles ($I_D = 0$ and $I_{DO} = 0$), occurring at winter solstice of approximately 5° as can be seen from Figures 1 and 2 (or 3).

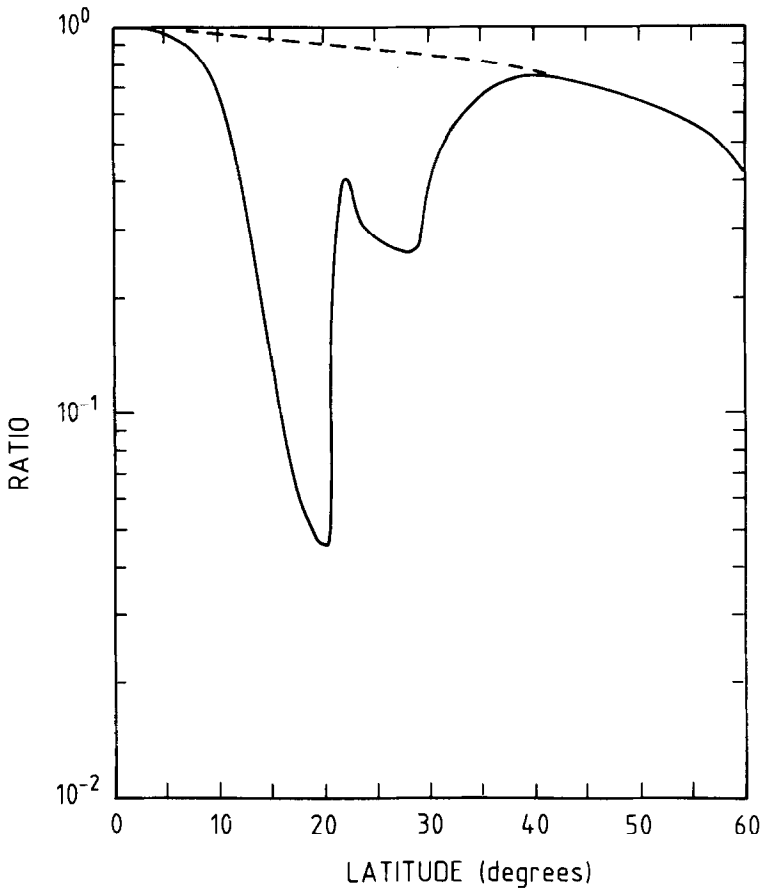

Fig. 5. Latitudinal variation in the winter hemisphere at a solar longitude of 45° (225°) of the ratio of the daily insolation with the oblateness effect and the effect of the ring system ($I_{DO\tau}$) to the daily insolation without the above mentioned effects (I_D) (full line). The ratio (I_{DO}/I_D) is also represented (dashed curve).

Comparing our results with those of Brinkman and McGregor (1979) we should note that the general pattern of the insolation curves is in reasonable agreement, although near the solstices and for low- and midlatitudes there are some striking differences particularly for the isocontours 1 and 2 cal cm^{-2} (Saturnian day)$^{-1}$. The higher optical depths used in our paper evidently yield attenuations of the solar radiation which are higher than those obtained by the above cited authors, who, for the optical thicknesses of the A, B, and C ring used 0.5, 1.0, and 0.1 respectively.

3.2. Mean daily insolation

The mean (summer, winter, or annual) daily insolations $\bar{I}_D$, $\bar{I}_{DO}$ and $\bar{I}_{DO\tau}$ as a function of latitude are plotted in Figures 7 and 9 (northern hemisphere) and in Figure 11 (both hemispheres), whereas the percentage differences $100\,(\bar{I}_{DO\tau} - \bar{I}_D)/\bar{I}_D$

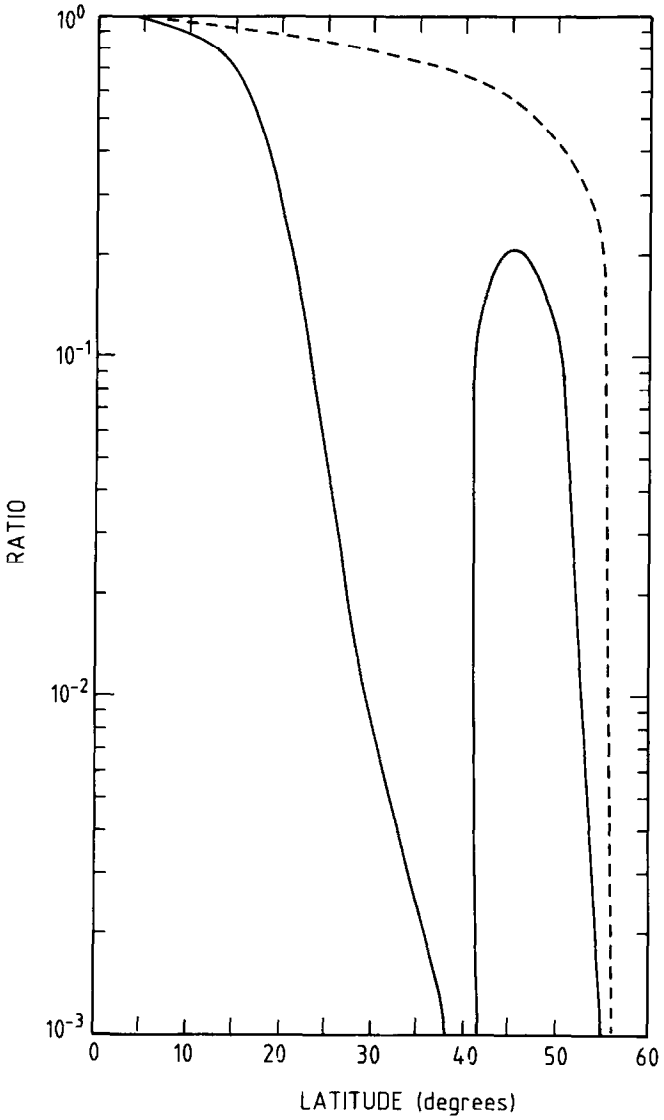

Fig. 6. Latitudinal variation in the winter hemisphere at winter solstice of the ratio of the daily insolation with the oblateness effect and the effect of the ring system (I_{DO_τ}) to the daily insolation without the above mentioned effects (I_D) (full line). The ratio (I_{DO}/I_D) is also represented (dashed curve).

and 100 $(\bar{I}_{DO} - \bar{I}_D)/\bar{I}_D$ are illustrated in Figures 8, 10, and 12. In Figures 10 and 12 the percentage difference $100(\bar{I}_{DO_\tau} - \bar{I}_{DO})/\bar{I}_{DO}$ is also shown. As in Section 2, the bars over symbols signify seasonal (denoted by S and W for summer and winter) or annual (A) averages.

The summer hemispheres being not affected by the ring system, it is obvious that $(\bar{I}_{DO_\tau})_S = (\bar{I}_{DO})_S$. The increase of insolation between a spherical and an oblate planet

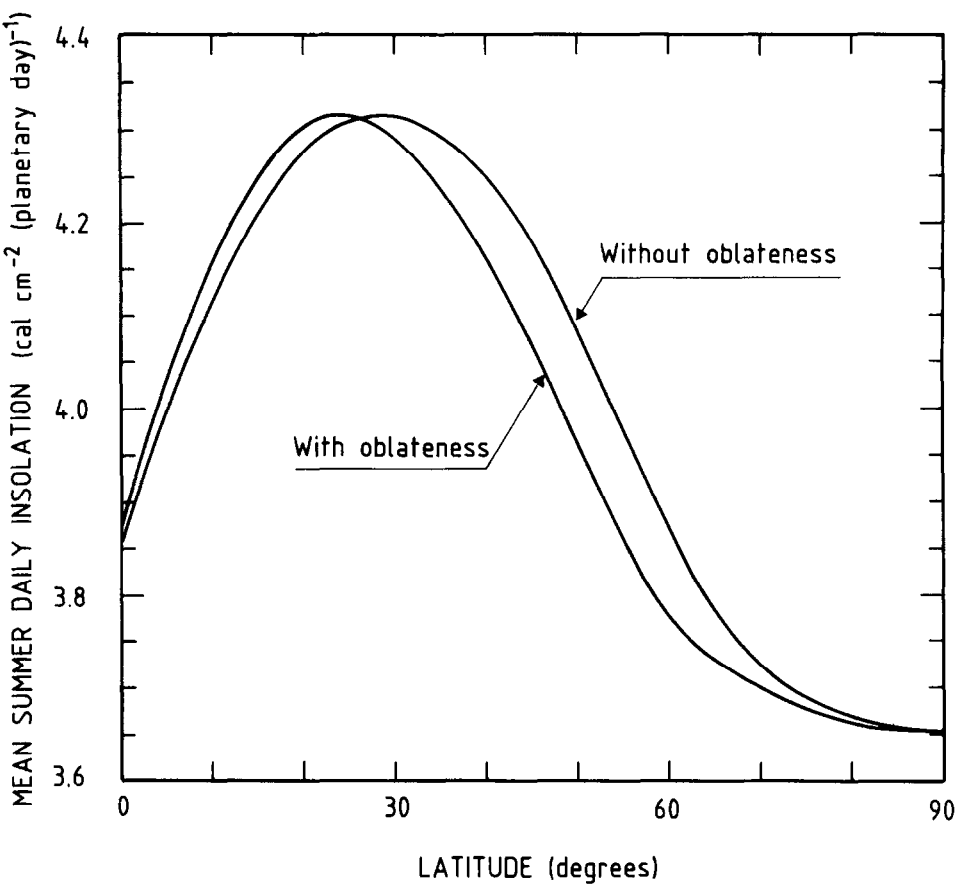

Fig. 7. Latitudinal variation of the mean summer daily insolations $(\bar{I}_{DO})_S$ (with oblateness) and $(\bar{I}_D)_S$ (without oblateness) at the top of the atmosphere of Saturn.

Saturn for latitudes less than the subsolar point (26°73) is clearly demonstrated in Figures 7 and 8 (see also Van Hemelrijck, 1982a), the maximum difference occurring at a latitude of about 12° and reaching a value of the order of 1%. Beyond the subsolar point, $(\bar{I}_{DO_7})_S = (\bar{I}_{DO})_S < (\bar{I}_D)_S$ and the maximum loss of insolation is found at mid-latitudes (50–55°) and is near 3%.

The mean winter daily insolations are depicted in Figure 9, the corresponding percentage differences in Figure 10. Comparing the mean winter isolations between a spherical and an oblate planet it can be seen from Figure 10 that the percentage difference increases with increasing latitude up to about 60° and may attain values of about 36%. At higher latitudes the differences remain practically constant. The importance of the shadow effect on the mean winter daily insolation is particularly evident from the Figure. For latitudes between 0 and about 20° the loss of insolation enhances to approximately 50%, then decreases to about 36% at 45° and finally keeps a nearly constant value up to polar region latitudes where it drops extremely

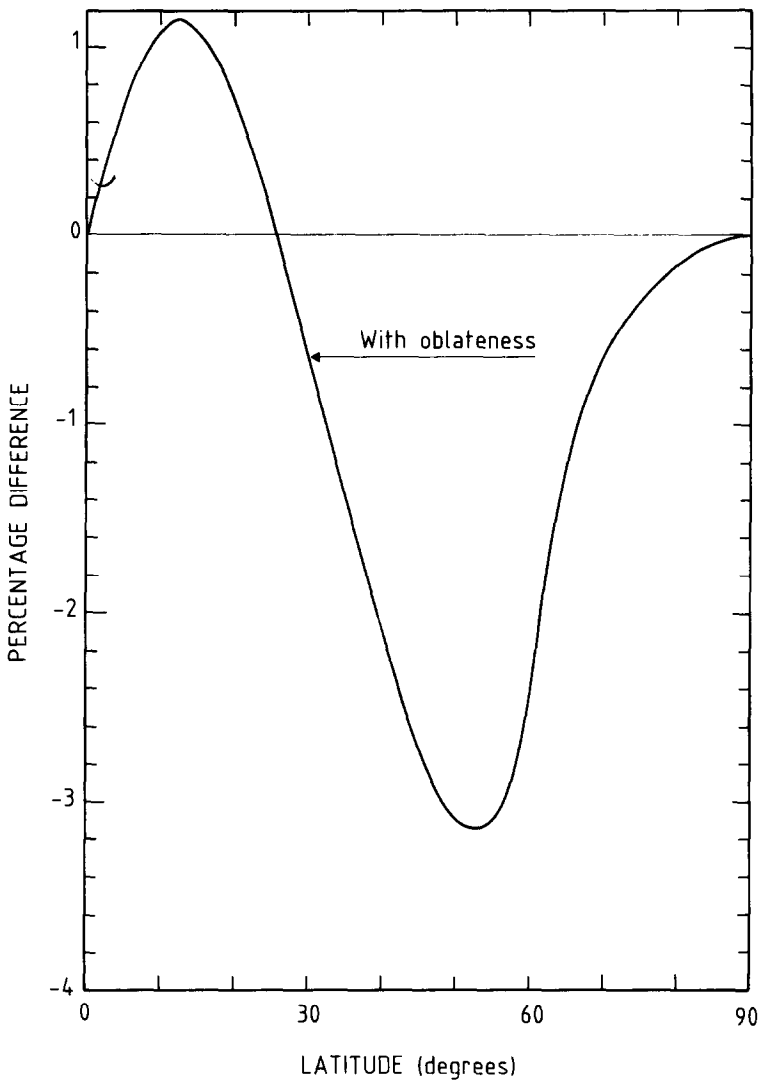

Fig. 8. Latitudinal variation of the percentage difference 100 $[(\bar{I}_{DO})_S - (\bar{I}_D)_S]/(\bar{I}_D)_S$. The bars over symbols signify seasonal averages.

rapid to zero. It is worth noting that poleward of 62°, the two curces representing the mean wintertime insolation coincide, the ring effect being equal to zero. For the sake of completeness, the effect of the rings only is also illustrated by the curve denoted by 'with rings'. The peak percentage difference attains a value of about 46% at $\lambda_\odot = 20°$ and the latitude past which the loss of solar energy due to the oblateness effect is greater than the reduction by the ring effect is near 40°.

It is to be emphasized that the Figures 7 and 9 relate to the northern hemisphere. In order to obtain the corresponding values for the southern one, the ordinates of

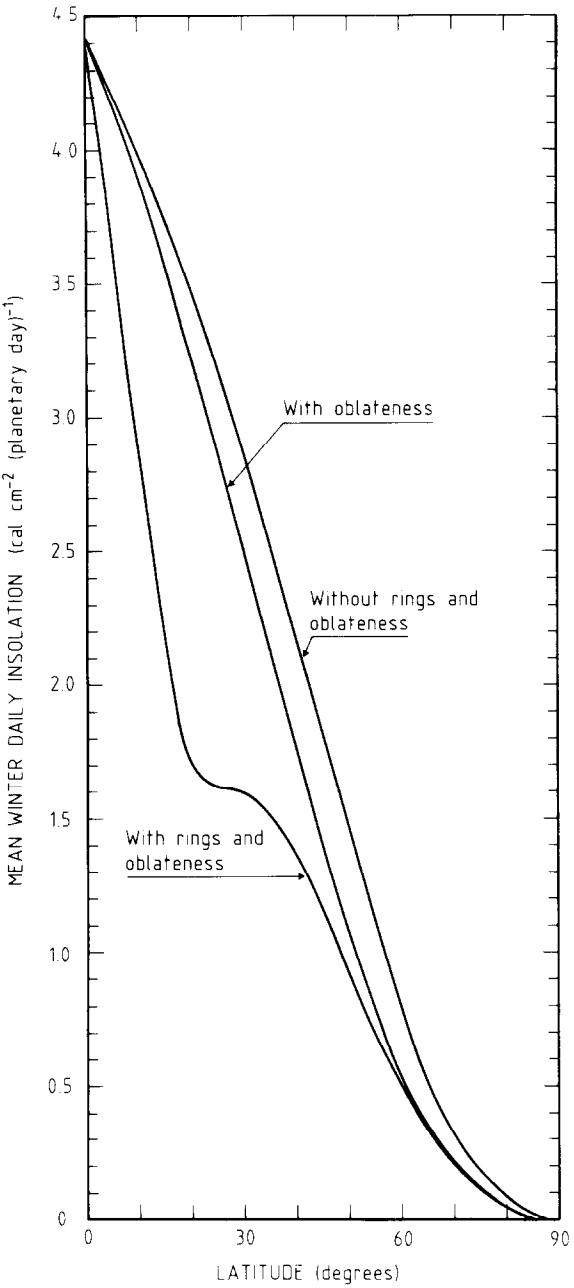

Fig. 9. Latitudinal variation of the mean winter daily insolations $(\bar{I}_{DO_T})_W$ (with rings and oblateness), $(\bar{I}_{DO})_W$ (with oblateness) and $(\bar{I}_D)_W$ (without rings and oblateness) at the top of the atmosphere of Saturn.

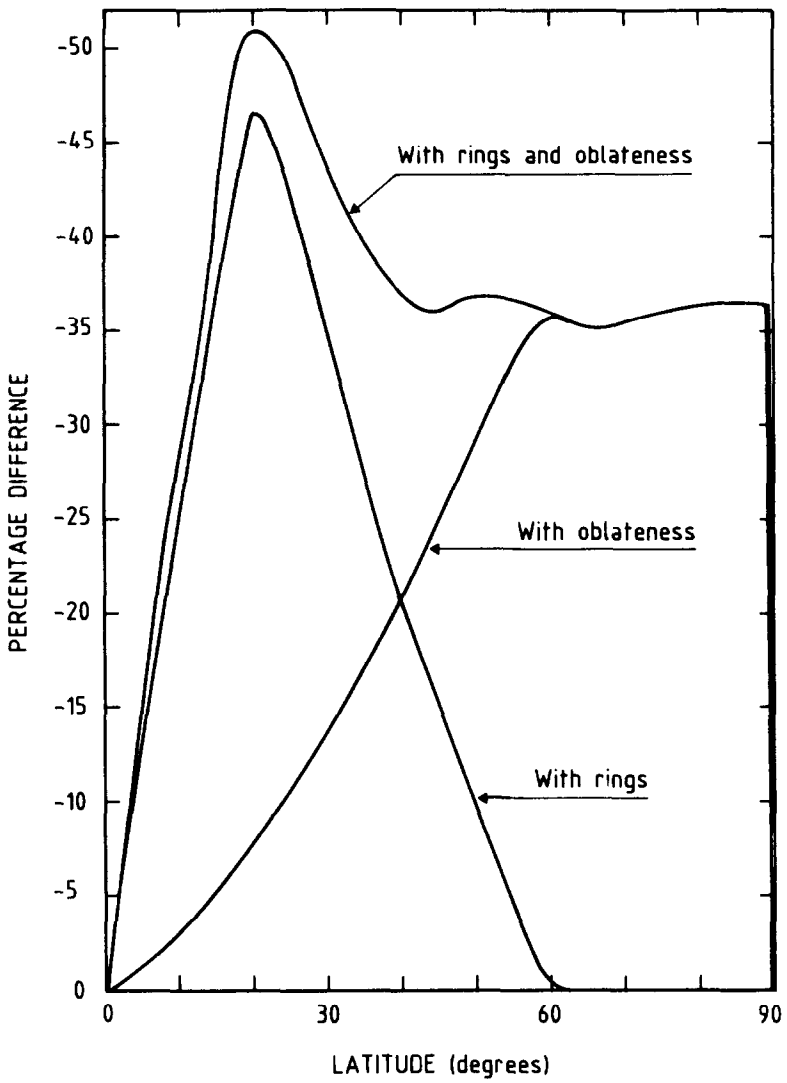

Fig. 10. Latitudinal variation of the percentage differences $100[(\bar{I}_{DO_T})_W - (\bar{I}_D)_W)]/(\bar{I}_D)_W$ (with rings and oblateness) and $100[(\bar{I}_{DO})_W - (\bar{I}_D)_W]/(\bar{I}_D)_W$ (with oblateness). The effect of the rings only is illustrated by the third curve denoted by 'with rings'.

Figure 7 have to be multiplied by the ratio T_S (northern hemisphere)/T_S (southern hemisphere) which equals approximately 1.15, whereas the data of Figure 9 have to be multiplied by the factor T_W (northern hemisphere)/T_W (southern hemisphere) which amounts about 0.87. Since the percentage differences are symmetric with respect to the planet's equator, a value at a given latitude in Figures 8 and 10 applies to both hemispheres.

The variability of the mean annual daily insolations as a function of latitude is shown in Figure 11; the corresponding percentage differences are plotted in Figure

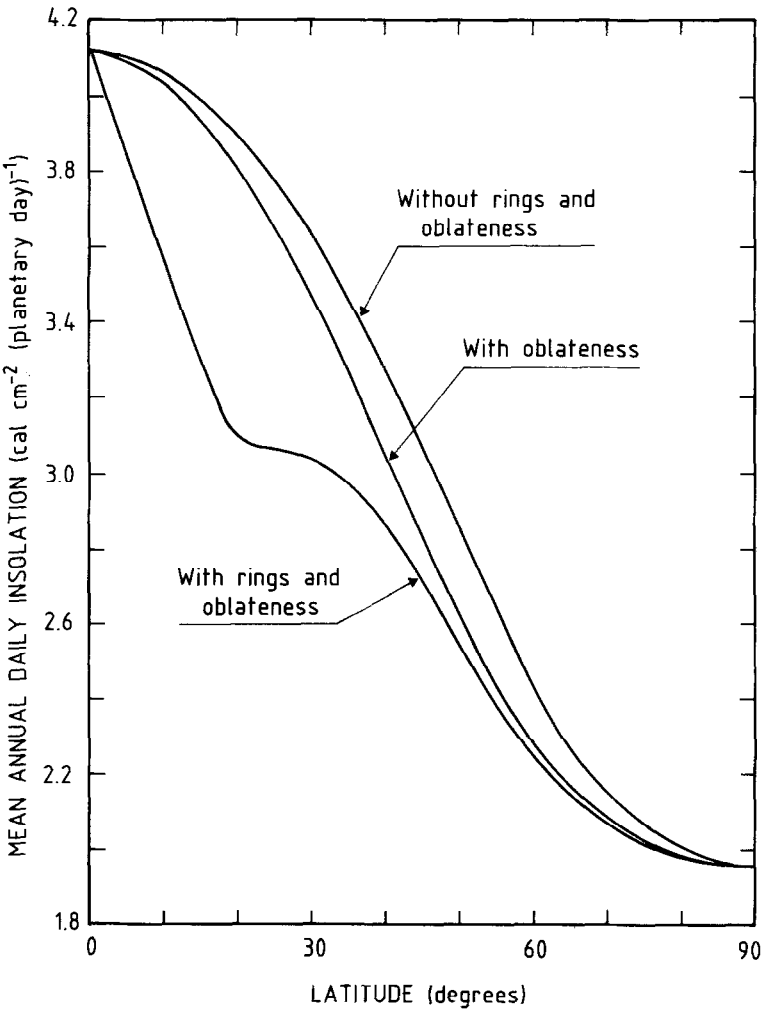

Fig. 11. Latitudinal variation of the mean annual daily insolations $(\bar{I}_{DOr})_A$ (with rings and oblateness), $(\bar{I}_{DO})_A$ (with oblateness) and $(\bar{I}_D)_A$ (without rings and oblateness) at the top of the atmosphere of Saturn.

12. Note that the data from both Figures are valid for the northern as well as for the southern hemisphere. The difference between the mean annual daily insolations $(\bar{I}_D)_A$ and $(\bar{I}_{DO})_A$ increases with increasing latitude and reaches a peak value of about 9% at a latitude of about 50°. Past of this latitude, the percentage difference reduces. The importance of the combined effect (rings + oblateness) on the mean annual daily insolation is particularly evident from Figure 12 where it can be seen that the percentage difference is strongly dependent upon the latitude. From 0 to 20°, the loss of insolation enhances nearly linear up to a maximum value of approximately 20% (18% when taking only into account the rings). In their 1979 paper Brinkman and McGregor have noted that 'for latitudes between 0 and 30° as much as 14% of

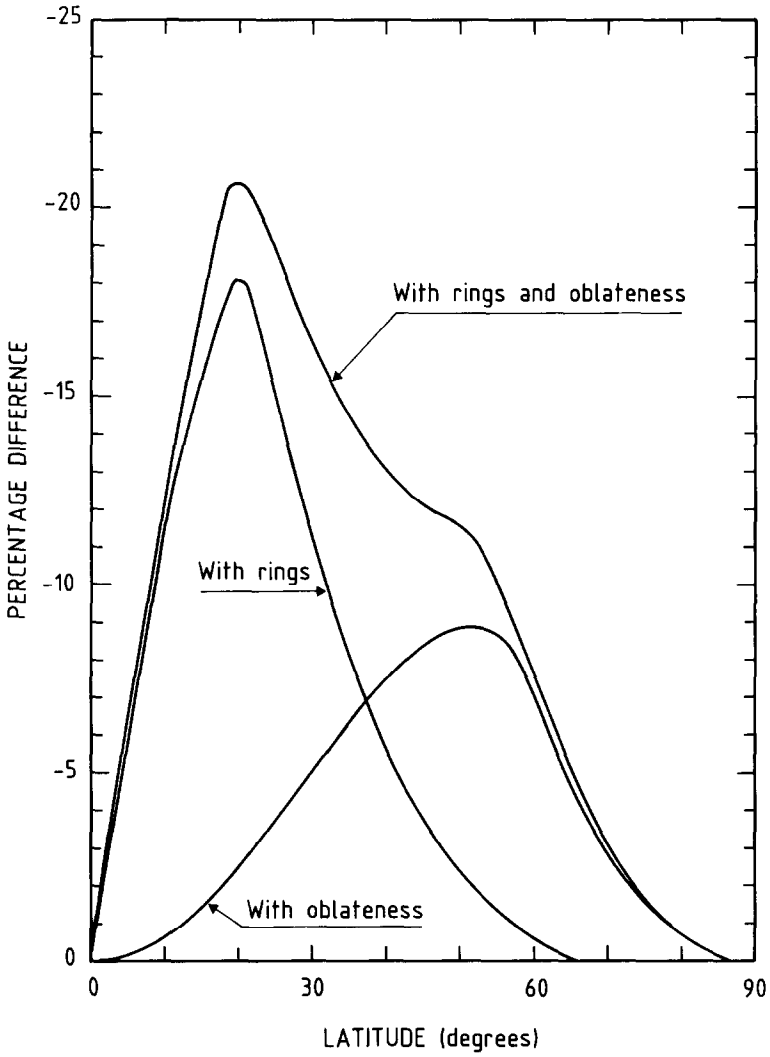

Fig. 12. Latitudinal variation of the percentage differences $100[(\bar{I}_{DO\tau})_A - (\bar{I}_D)_A]/(\bar{I}_D)_A$ (with rings and oblateness) and $100(\bar{I}_{DO})_A - (\bar{I}_D)_A]/(\bar{I}_D)_A$ (with oblateness). The effect of the rings only is illustrated by the third curve denoted by 'with rings'.

the total annual insolation is lost through the shadow effect'. At 30, 40, and 50° we found, for the combined effect, percentage differences of 16.6, 13.1, and 11.4% (the corresponding values for which only the rings are responsible amount to about 11.8, 5.6, and 2.1%). Based on the graph figuring int he paper of the above mentioned authors we get the impression that their values are considerably lower. Figure 12 also clearly indicates that the influence of the shadow is almost negligible between 55 and 65° (equal or less than about 1%). Finally, near 37° the influence of the oblateness is numerically equal to the effect of the ring shadow (~7%).

4. Concluding Remarks

This study clearly demonstrates that the shadow of the ring system of Saturn causes significant variations in both the planetary-wide distribution and the intensity of the daily insolation. The combined effect of the ring shadows and the oblateness decreases the daily solar radiation over much of the winter hemispheres mainly near the solstices (up to mid-latitudes). In the vicinity of the equinoxes the loss of solar energy is principally limited to equatorial and low latitude regions. Furthermore, it is obvious that the summer hemispheres are not affected by the rings.

Concerning the mean winter and annual daily insolations it is found that the reduction reaches peak values of respectively 50 and 20% at a latitude of 20°.

Acknowledgements

We would like to thank L. Vastenaekel, J. Schmitz and F. Vandreck for their help with the manuscript and the illustrations. The computer assistance of A. Pittonvils and E. Falise is also very much appreciated.

References

Allen, C. W.: 1963, *Astrophysical Quantities* (2nd ed.), Athlone Press, University of London.
Brinkman, A. W. and McGregor, J.: 1979, *Icarus* **38**, 479.
Cook, A. F., Franklin, F. A., and Palluconi, F. D.: 1973, *Icarus* **18**, 317.
Davies, M. E., Abalakin, V. A., Lieske, J. H., Seidelmann, P. K., Sinclair, A. T., Sinzi, A. M., Smith, B. A., and Tjuflin, Y. S.: 1983, *Celest. Mech.* **29**, 309.
Esposito, L. W., O'Callaghan, M., and West, R. A.: 1983, *Icarus* **56**, 439.
Levine, J. S., Kraemer, D. R., and Kuhn, W. R.: 1977, *Icarus* **31**, 136.
Smith, B. A., Soderblom, L., Beebe, R., Boyce, J., Briggs, G., Bunker, A., Collins, S. A., Hansen, C. T., Johnson, T. V., Mitchell, J. L., Terrile, R. J., Carr, H., Cook, A. F., II, Cuzzi, J., Pollack, J. B., Danielson, G. E., Ingersoll, A., Davies, M. E., Hunt, G. E., Masursky, H., Shoemaker, E., Morrison, D., Owen, T., Sagan, C., Veverka, J., Strom, R., and Suumi, V. E.: 1981, *Science* **212**, 163.
Van Hemelrijck, E.: 1982a, *Icarus* **51**, 39.
Van Hemelrijck, E.: 1982b, 'The Oblateness Effect on the Solar Radiation Incident at the Top of the Atmosphere of Mars', in *Proceedings of the Workshop on the Planet Mars*, Leeds, 1982, ESA Special Publication SP-185, p. 59.
Van Hemelrijck, E.: 1982c, *Bull. Acad. R. Belg., Cl. Sci.* **68**, 675.
Van Hemelrijck, E.: 1983a, *Solar Energy* **31**, 223.
Van Hemelrijck, E.: 1983b, *The Moon and the Planets* **28**, 125.
Van Hemelrijck, E.: 1985a, *Earth, Moon, and Planets* **33**, 157.
Van Hemelrijck, E.: 1985b, *Earth, Moon, and Planets* **33**, 163.
Vorob'yev, V. I. and Monin, A. S.: 1975, *Atm. Ocean. Phys.* **11**, 557.
Ward, W. R.: 1974, *J. Geophys. Res.* **79**, 3375.
Willson, R. C.: 1982, *J. Geophys. Res.* **87**, 4319.